Organic Letters

Supporting Information for

Title: Biased Helical Folding of Chiral Oligoindole Foldamers

Veluru Ramesh Naidu, Min Cheol Kim, Jae-min Suk, Ho-Joong Kim, Myongsoo Lee,

Eunji Sim,* and Kyu-Sung Jeong*

Center of Bioactive Molecular Hybrids and Department of Chemistry, Yonsei University, Seoul-120-749 South Korea

ksjeong@yonsei.ac.kr

Contents

1. Synthesis and Characterization

General: All chemicals were purchased from commercial suppliers and used without further purification unless otherwise specified. E_3N and CH_2Cl_2 were purified by drying over CaH_2, followed by distillation, and tetrahydrofuran was distilled from sodium and benzophenone. The chemical shifts of ^1H NMR and ^{13}C NMR spectra are reported using the solvent signal as an internal reference, DMSO-d_6 (2.50 ppm for ^1H NMR and 39.5 ppm for ^{13}C NMR). The column chromatography was performed using 230-400 mesh ultra pure silica. UV-visible absorption spectra were recorded on Agilent 8453 UV-visible spectrophotometer. ^1H NMR and ^{13}C NMR spectra were obtained on Bruker 400 MHz spectrometer. MALDI-TOF mass spectrometric measurements were performed on Voyager-DE^{TM} STR Biospectrometry Workstation MALDI-TOF. Circular dichroism (CD) spectra were conducted on a JASCO J-810 spectropolarimeter. Melting points were determined with a Barnsted Electrochemical (IA9100) and were not corrected. The elemental analysis data were obtained from the National Center for Inter-University Research Facilities at the Seoul National University.

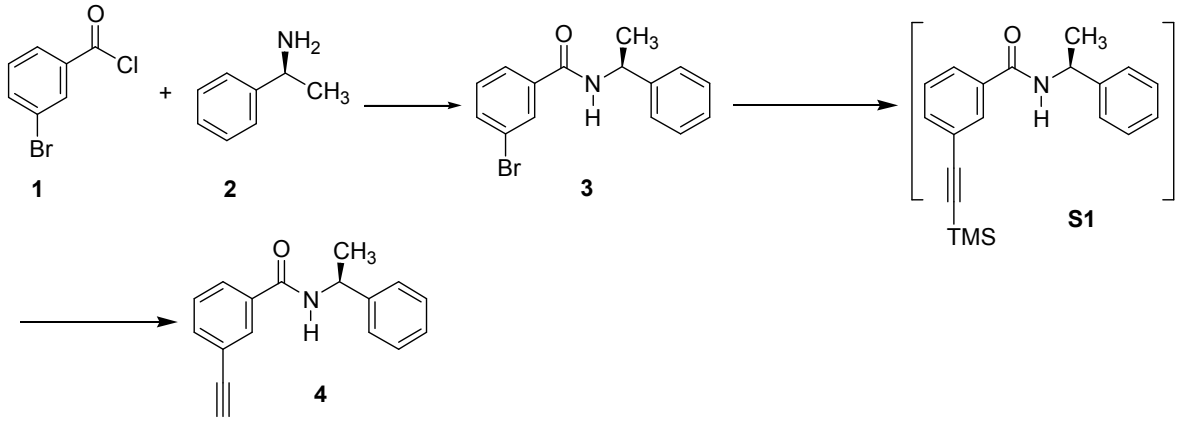

Compound **3**: Oxallyl chloride (8.5 g, 67.1 mmol) and a catalytic amount of DMF were added to a stirred solution of 3-bromobenzoic acid (4.5 g, 22.4 mmol) in CH_2Cl_2 (20 mL) at

0 ^{o}C (ice-water bath) for 1 h under nitrogen atmosphere, and the solution was concentrated under reduced pressure. The residue was dissolved in anhydrous CH_2Cl_2 (5 mL) and slowly transferred to a CH_2Cl_2 solution (5 mL) at 0 ^{o}C containing (*S*)-phenylethylamine (2.7 g, 22.4 mmol) and pyridine (0.5 mL). After stirring for 6 h (0 ^{o}C to room temperature), the mixture was diluted with CH_2Cl_2 (20 mL), washed with saturated $NaHCO_3$ solution and brine, and dried over anhydrous Na_2SO_4. After concentration, the residue was purified by column chromatography (silica gel, hexane/EtOAc = 5:3) to give **3** (6.2 g, 92%) as a white solid. Mp: 117-118 ^{o}C. ^{1}H NMR (400 MHz, DMSO-d_6): δ 8.93 (d, J = 8.0 Hz, 1H), 8.09 (s, 1H), 7.88 (d, J = 8.0 Hz, 1H), 7.73 (d, J = 8.0 Hz, 1H), 7.43 (t, J = 7.8 Hz, 1H), 7.38 (m, 2H), 7.32 (t, J = 7.3 Hz, 2H), 7.22 (t, J = 7.2 Hz, 1H), 5.16 (qn, J = 7.3 Hz, 1H), 1.48 (d, J = 7.1 Hz, 3H). ^{13}C NMR (100 MHz, DMSO-d_6): δ 163.9, 144.6, 136.6, 133.9, 130.5, 129.9, 128.2, 126.6, 126.6, 126.0, 121.6, 48.6, 22.1. IR (thin film): 3285(NH), 1638(C=O) cm^{-1}. MALDI-TOF MS: calcd for $C_{15}H_{14}Br$ NO $[MH]^+$ = 304.03, found, $[MH]^+$ = 304.09. Anal. Calcd for $C_{15}H_{14}Br$ NO: C, 59.23; H, 4.64; N, 4.60. Found: C, 59.36; H, 4.70; N, 4.63. The identical procedure was followed by using (*R*)-phenylethylamine to prepare the enantiomer of **3** (ent-**3**) in 93% yield.

Compound 4:[1] **3** (5.0 g, 16.4 mmol), Pd (dba) $_2$ (0.23 g, 0.41 mmol), pph$_3$ (0.43 g, 1.64 mmol) and CuI (0.08 g, 0.41 mmol) were mixed in a 50 mL schlenk flask under nitrogen. The flask was then evacuated under vacuum and backfilled with N_2, which process was repeated three times. After addition of degassed Et_3N (35 mL), THF (15 mL), and

[1] (a) Sonogashira, K. In Metal-Catalyzed Cross-Coupling Reactions; Diederch, F.; Stang, P. J. Eds.; Wiley: Weinheim (Germany), **1997**; Chapter 5, pp 203-229. (b) Zhang, J.; Pesak, D. J.; Ludwick, J. L.; Moore, J. S. *J. Am. Chem. Soc.* **1994**,*116*, 4227-4239. (c) Erdelyi, M.; Gogoll, A. *J. Org. Chem.* **2001**, *66*, 4165-4169.

trimethylsilyl-ethyne (5.5 g, 56.2 mmol), the rubber stopper was replaced with screw stopper (screw cock) under nitrogen. The solution was stirred at 53-55 ^{o}C for 16 h. The resulting suspension was allowed to reach room temperature and filtered through Celite pad. After concentration, the residue was purified by flash column chromatography (silica gel, hexane/EtOAc = 5:3) to give **S1**. ^{1}H NMR (400 MHz, DMSO-d_6): δ 8.93 (d, J = 8.0 Hz, 1H), 8.02 (s, 1H), 7.89 (d, J = 7.8 Hz, 1H), 7.59 (d, J = 7.6 Hz, 1H), 7.46 (t, J = 7.7 Hz, 1H), 7.38 (m, 2H), 7.32 (t, J = 7.4 Hz, 2H), 7.22 (t, J = 7.2 Hz, 1H), 5.17 (qn, J = 7.2 Hz, 1H), 1.48 (d, J = 6.8 Hz, 3H). ^{13}C NMR (100 MHz, DMSO-d_6): δ 164.5, 144.7, 134.8, 134.1, 130.0, 128.8, 128.3, 128.2, 126.6, 126.0, 122.1, 104.6, 94.8, 48.6, 22.1, 0.1.

Compound **S1** (4.5 g, 14 mmol) was dissolved in MeOH (60 mL), to which solution a catalytic amount of K_2CO_3 (0.4 g, 2.8 mmol) was added. After stirred for 30 min, the mixture was concentrated under reduced pressure, and then CH_2Cl_2 was added. The solution was washed with H_2O and brine, and dried over anhydrous $MgSO_4$. After concentration, the residue was purified by column chromatography (silica gel, hexane/EtOAc = 7:3) to give **4** (3.3 g, 81% for two steps) as a white solid. Mp: 137-138 ^{o}C. ^{1}H NMR (400 MHz, DMSO-d_6): δ 8.91 (d, J = 7.6 Hz, 1H), 8.01 (s, 1H), 7.90 (d, J = 8.0 Hz, 1H), 7.63 (d, J = 7.6 Hz, 1H), 7.49 (t, J = 7.6 Hz, 1H), 7.38 (d, J = 7.3 Hz, 2H), 7.32 (t, J = 7.4 Hz, 2H), 7.22 (t, J = 7.2 Hz, 1H), 5.16 (qn, J = 7.3 Hz, 1H), 4.28 (s, 1H), 1.48 (d, J = 7.1 Hz, 3H). ^{13}C NMR (100 MHz, DMSO-d_6): δ 164.5, 144.7, 134.9, 134.2, 130.3, 128.8, 128.2, 128.1, 126.6, 126.0, 121.7, 82.9, 81.4, 48.6, 22.2. IR (thin film): 3313(C(sp)-H), 3273(NH), 1634(C=O) cm^{-1}. $C_{17}H_{15}NO$ $[MH]^+$ = 250.12, found, $[MH]^+$ = 250.15. Anal. Calcd for $C_{17}H_{15}NO$: C, 81.90; H, 6.06; N, 5.62. Found: C, 81.90; H, 6.00; N, 5.63. The

identical procedure was followed to prepare the enantiomer of **4** (ent-**4**) from ent-**3** in 92% yield for two steps.

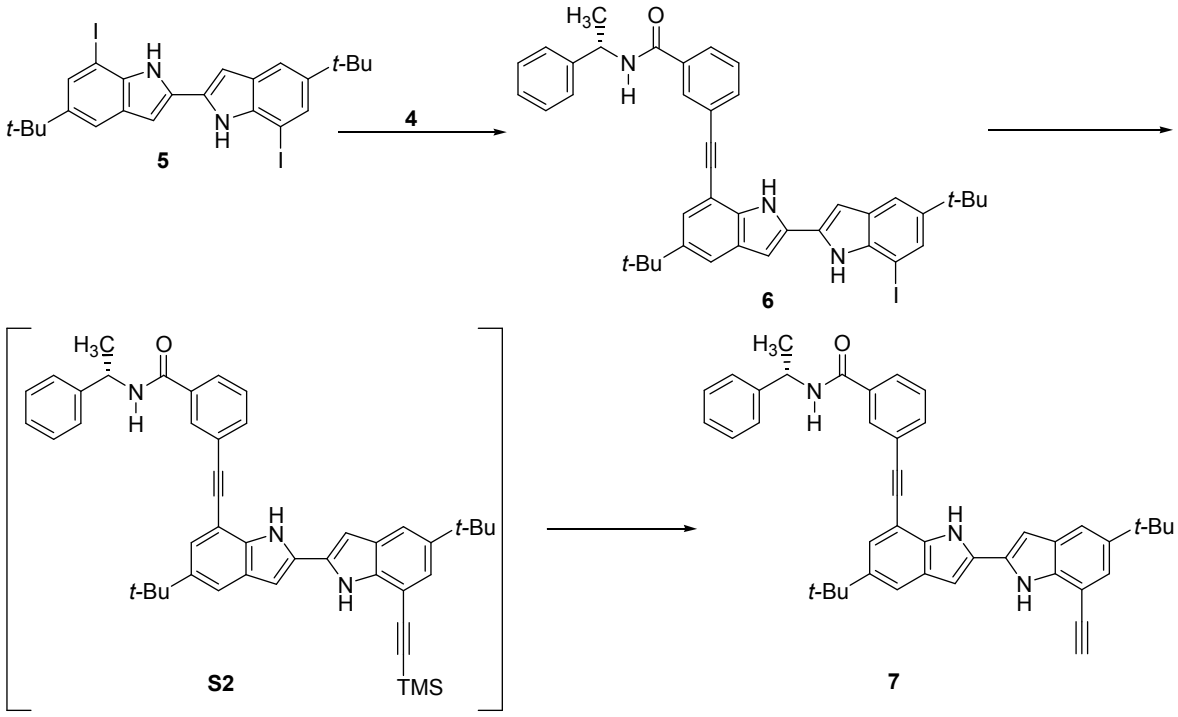

Compound 6: The synthesis of 5,5′-di(*tert*-butyl)-7,7′-diiodo-2,2′-biindolyl (**5**) was described previously.[2] Compound 5 (3.4 g, 5.7 mmol), Pd (dba) $_2$ (55 mg, 0.095 mmol), pph_3 (0.1 g, 0.38 mmol), and CuI (18 mg, 0.095 mmol) were added to a schlenk flask under N_2. The Schlenk flask was fitted with a rubber stopper, and evacuated under vacuum and back-filled with N_2 (repeated three times). After addition of degassed Et_3N (20 mL), THF (30 mL), and compound **4** (0.95 g, 3.81 mmol), the rubber stopper was replaced with a screw stopper and the solution was stirred at 53-55 ^oC for 16 h. The resulting suspension was allowed to cool down room temperature, filtered through Celite pad and concentrated.

[2] Chang, K.-J.; Moon, D.; Lah, M. S. and Jeong, K.-S. *Angew. Chem., Int. Ed.*, **2005,** *44,* 7926-7929.

The residue was dissolved in CH_2Cl_2 (100 mL), washed with saturated $NaHCO_3$ solution and brine, and dried over anhydrous Na_2SO_4. After concetration, the residue was purified by column chromatography (silica gel, hexane/EtOAc = 7:3) to give **6** (1.64 g, 60%) as a white solid. Mp: 213-214 ^oC. ^1H NMR (400 MHz, DMSO-d_6): δ 11.56 (s, 1H), 11.02 (s, 1H), 8.99 (d, J = 8.0 Hz, 1H), 8.29 (s, 1H), 7.95 (d, J = 7.6 Hz, 1H), 7.90 (d, J = 8.0 Hz, 1H), 7.63 (s, 1H), 7.60 (t, J = 7.8 Hz, 1H), 7.55 (s, 2H), 7.43 (m, , 3H), 7.34 (t, J = 7.6 Hz, 2H), 7.23 (m, , 2H), 7.19 (s, 1H), 5.21 (qn, J = 7.4 Hz, 1H), 1.51 (d, J = 7.2 Hz, 3H), 1.37 (s, 9H), 1.33 (s, 9H),. ^{13}C NMR (100 MHz, DMSO-d_6): δ 164.8, 144.7, 144.4, 142.4, 137.1, 135.2, 135.0, 134.1, 131.8, 131.7, 131.6, 130.3, 129.1, 128.8, 128.8, 128.7, 128.3, 127.8, 126.7, 126.1, 123.9, 123.0, 117.6, 116.0, 104.6, 101.6, 101.2, 92.0, 87.7, 76.2, 48.7, 34.3, 34.2, 31.7, 31.6., 22.2. IR (thin film): 3297(NH), 1634(C=O) cm^{-1}. MALDI-TOF MS: calcd for $C_{41}H_{40}IN_3O$ $[M]^+$ = 717.22, found, $[M]^+$ = 717.39, Anal. Calcd for $C_{41}H_{40}IN_3O$: C, 68.62; H, 5.62; N, 5.86. Found: C, 68.60; H, 5.61; N, 5.81. The identical procedure was followed to prepare ent-**6** (63%) from ent-**4**.

Compound 7: 6 (0.80 g, 1.1 mmol), Pd (dba) $_2$ (16 mg, 0.028 mmol), PPh_3 (29 mg, 0.11 mmol) and CuI (6 mg, 0.028 mmol) were added to a 50 mL schlenk flask under an atmosphere of N_2. The flask was fitted with a rubber stopper, and then evacuated under vacuum and back-filled with N_2 (repeated three times). After addition of degassed Et_3N (20 mL), THF (15 mL) and trimethylsilyl-ethyne (0.47 mL, 0.33 mmol), the solution was stirred at 53-55 ^oC for 18 h. The work-up is the same as that for compound **6**. The product was purified by column chromatography (silica gel, hexane/EtOAc = 4:1) to give **S2** (0.65 g, 85%) as an oil: ^1H NMR (400 MHz, DMSO- d_6): δ 11.55 (s, 1H), 11.23 (s, 1H), 8.97 (d,

J = 7.9 Hz, 1H), 8.27 (s, 1H), 7.93 (m, 2H), 7.64 (m, 2H), 7.56 (d, *J* = 7.6 Hz, 1H), 7.43 (m, 3H), 7.34 (t, *J* = 7.8 Hz, 1H), 7.29 (d, *J* = 1.77 Hz, 1H), 7.23 (t, *J* = 7.2 Hz, 2H), 7.15 (m, 2H), 5.23 (qn, *J* = 7.4 Hz, 1H), 1.51 (d, *J* = 7.12 Hz, 3H), 1.37 (s, 9H), 1.34 (s, 9H), 0.34 (s, 9H),. ^{13}C NMR (100 MHz, DMSO-d_6): δ 164.7, 144.8, 142.4, 142.3, 135.3, 135.2, 135.0, 134.0, 131.8, 131.7, 130.2, 128.7, 128.6, 128.6, 127.7, 126.6, 126.1, 124.2, 123.5, 123.0, 117.6, 117.6, 104.8, 104.5, 102.7, 101.0, 97.6, 92.1, 87.6, 48.6, 34.3, 34.2, 20.7, 0.1.

Compound **S2** (0.55 g, 0.8 mmol) was dissolved in MeOH (20 mL) and a catalytic amount of K_2CO_3 (0.05 g, 0.4 mmol) was added. After 30 min stirring, the mixture was concentrated and the residue was dissolved in CH_2Cl_2. The solution was washed with H_2O and brine, and dried over anhydrous $MgSO_4$. After concentration, the residue was purified by column chromatography (silica gel, hexane/EtOAc = 4:1) to give **7** (0.45 g, 91%) as a white solid. Mp: 195-196 ^{o}C. ^{1}H NMR (400 MHz, DMSO-d_6): δ 11.50 (s, 1H), 11.44 (s, 1H), 8.99 (d, *J* = 7.9 Hz, 1H), 8.29 (s, 1H), 7.92 (m, 2H), 7.60 (m, 3H), 7.43 (m, 3H), 7.34 (m, 3H), 7.23 (t, *J* = 7.6 Hz, 1H), 7.18 (s, 1H), 7.18 (s, 1H), 5.23 (qn, *J* = 7.4 Hz, 1H), 1.51 (d, *J* = 7.0 Hz, 3H), 1.37 (s, 9H), 1.34 (s, 9H). ^{13}C NMR (100 MHz, DMSO-d_6): δ 164.8, 144.8, 142.4, 142.2, 135.6, 135.2, 135.0, 134.1, 131.9, 131.9, 130.3, 128.8, 128.7, 128.6, 128.3, 127.7, 126.7, 126.1, 124.1, 123.8, 123.0, 123.5, 117.6, 117.4, 104.5, 104.2, 100.9, 100.8, 91.9, 87.6, 84.2, 81.3, 48.6, 34.3, 34.2, 29.4, 22.2. IR (thin film): 3301(NH), 2202(C≡C), 1642(C=O) cm^{-1}. MALDI-TOF MS: calcd for $C_{43}H_{41}N_3O$ $[M]^+$ = 615.32, found, $[M]^+$ = 615.52. Anal. Calcd for $C_{43}H_{41}N_3O$: C, 83.87; H, 6.71; N, 6.82. Found: C, 83.87; H, 6.90; N, 6.65. The identical procedure was followed to prepare ent-**7** (90% for two steps) from ent-**6**.

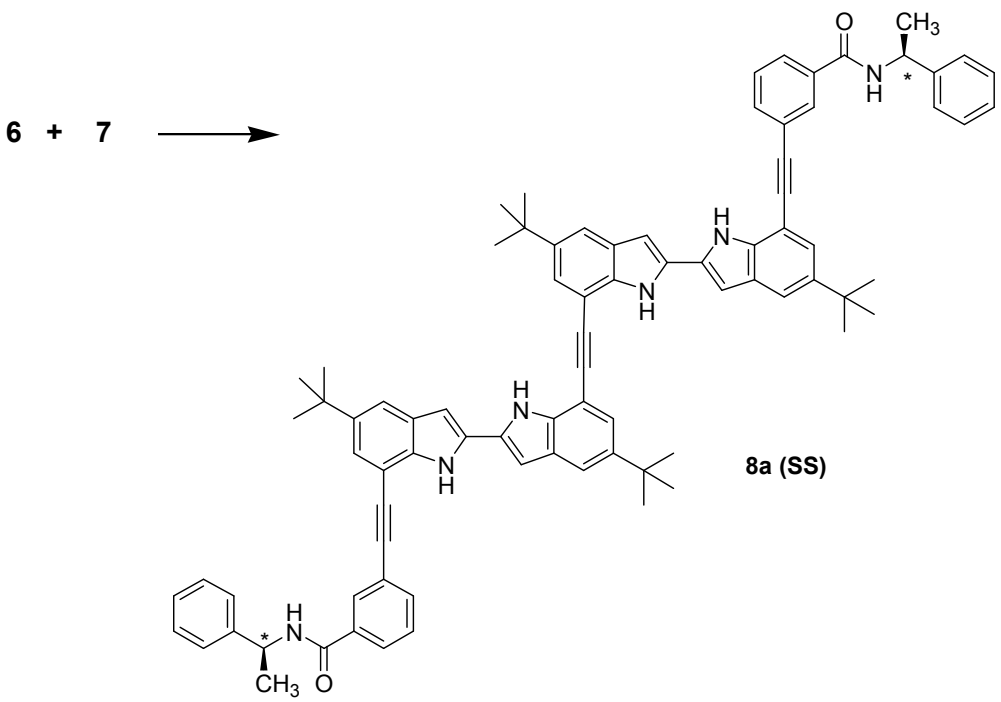

Compound 8a: 6 (0.31 g, 0.438 mmol), Pd (dba) $_2$ (7 mg, 0.011 mmol), pph$_3$ (12 mg, 0.044 mmol) and CuI (2 mg, 0.010 mmol) were mixed in a 50 mL schlenk flask under N_2. The flask was evacuated under vacuum and back-filled with N_2 (repeated three times). After addition of degassed Et_3N (10 mL), THF (15 mL), and **7** (0.27 g, 0.438 mmol), the solution was stirred at 53-55 ^oC for 18 h. The work-up is the same as that for **6**. The crude product was purified by column chromatography (silica gel, hexane/EtOAc = 5:1) to give **8a** (0.35 g, 66%) as a white solid. Mp: 242-243 ^oC. ^1H NMR (400 MHz, DMSO-d_6): δ 11.57 (s, 1H; NH), 11.54 (s, 1H; NH), 8.92 (d, J = 8.0 Hz, 1H), 8.23, (s, 1H), 7.89 (d, J = 7.8 Hz, 1H), 7.78 (d, J = 7.6 Hz, 1H), 7.66 (s, 2H), 7.59 (s, 1H), 7.48 (t, J = 7.6 Hz, 1H), 7.40 (m, 3H), 7.32 (t, J = 7.6 Hz, 2H), 7.21 (m, 3H), 5.18 (qn, J = 7.2 Hz, 1H), 1.48 (d, J = 6.8 Hz, 3H), 1.39 (s, 9H), 1.37 (s, 9H). ^{13}C NMR (100 MHz, DMSO-d_6): δ 164.7, 144.8, 142.4, 135.3, 135.1, 134.9, 134.0, 132.1, 131.9, 130.3, 128.8, 128.7, 128.6, 128.2, 127.6, 126.6, 126.1,

124.2, 123.8, 122.9,117.6, 117.2, 105.4, 104.5, 01.1, 101.0, 91.9, 90.1, 87.6, 48.6, 34.3, 34.2, 22.2. IR (thin film): 3420(NH), 1636(C=O) cm^{-1}. MALDI-TOF MS: calcd for $C_{84}H_{80}N_6O_2$ $[M]^+$ = 1204.63, found, $[M]^+$ = 1204.86.; **8a:** Anal. Calcd for $C_{84}H_{80}N_6O_2$: C, 83.69; H, 6.69; N, 6.97. Found: C, 83.75; H, 6.64; N, 6.92.

The identical procedure was followed to prepare **8b** (60%) from ent-**6** and ent-**7**. **8b**: MALDI-TOF MS: calcd for $C_{84}H_{80}N_6O_2$ $[M]^+$ = 1204.63, found, $[M]^+$ = 1204.85.; Anal. Calcd for $C_{84}H_{80}N_6O_2$: C, 83.69; H, 6.69; N, 6.97. Found: C, 83.64; H, 6.68; N, 6.91.

2. 2D ^{1}H-^{1}H COSY, TOCSY, and NOESY spectra

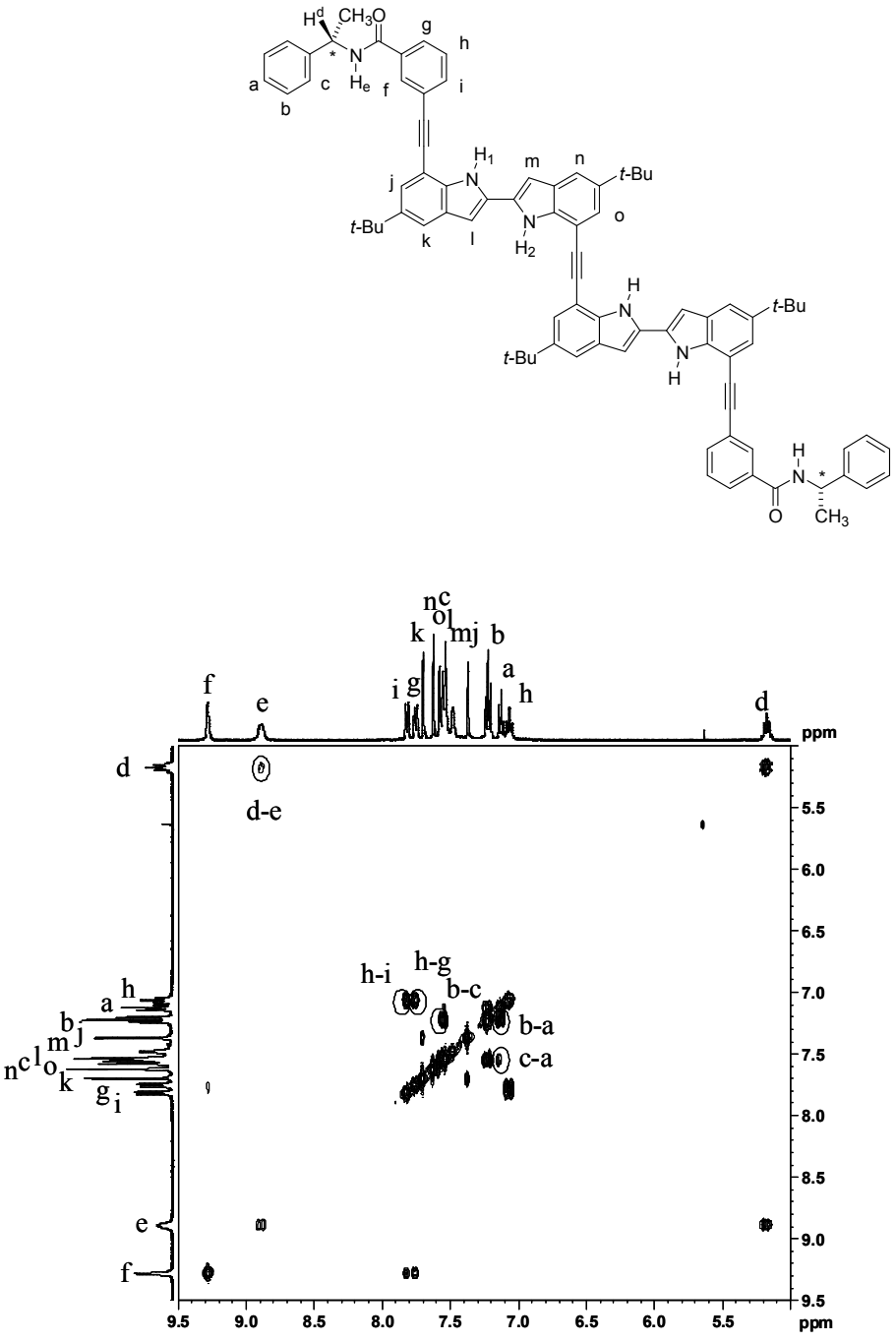

Figure S1. Partial COSY spectrum (400 MHz, 25 ^{o}C, acetone-d_6) for a mixture of **8a** (10 mM) and $TBA^{+}Cl^{-}$ (3 equiv).

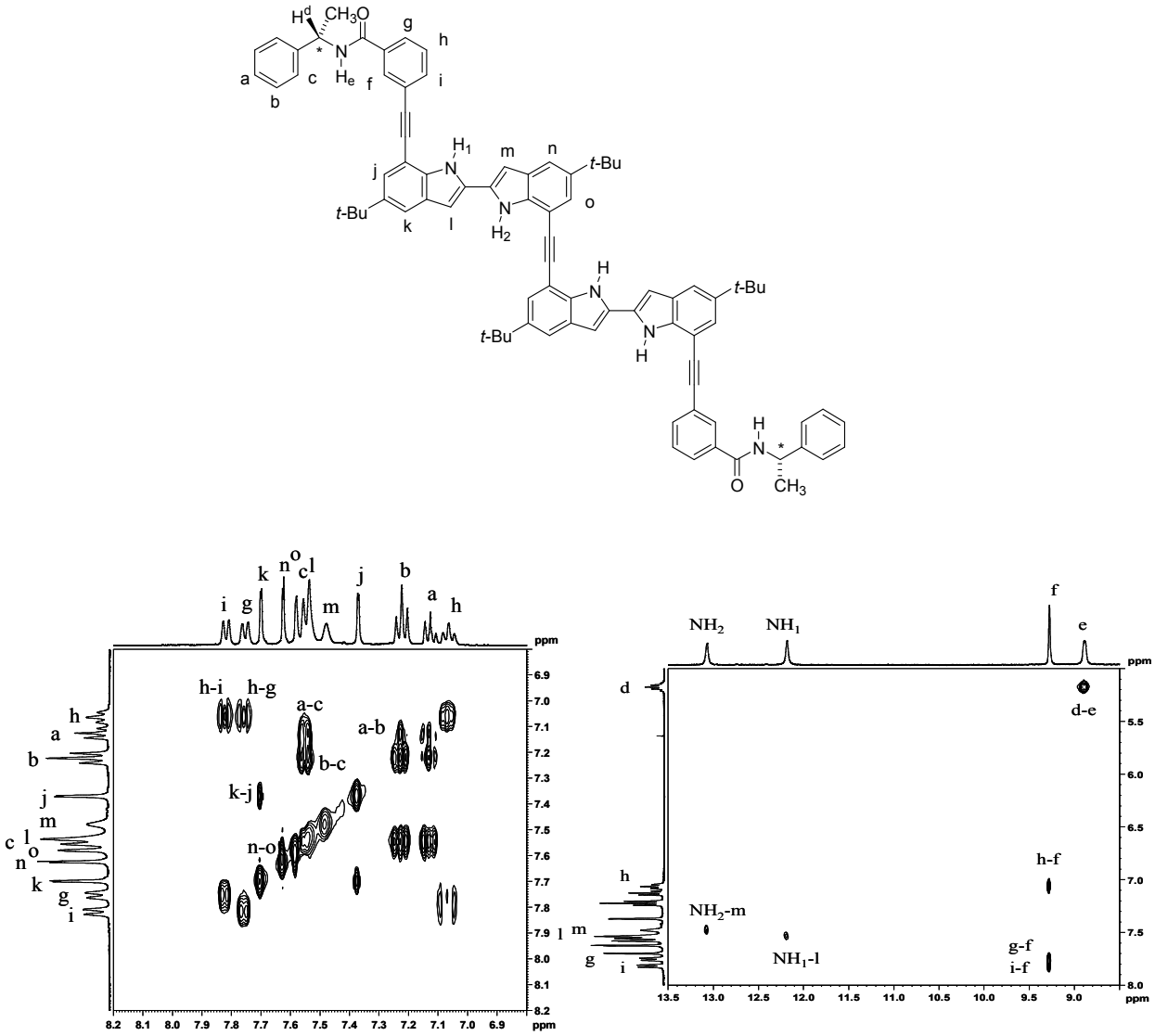

Figure S2. TOCSY spectra (400 MHz, 25 ^{o}C, acetone-d_6, mixing time = 60 ms) for a mixture of **8a** (10 mM) and $TBA^{+}Cl^{-}$ (3 equiv).

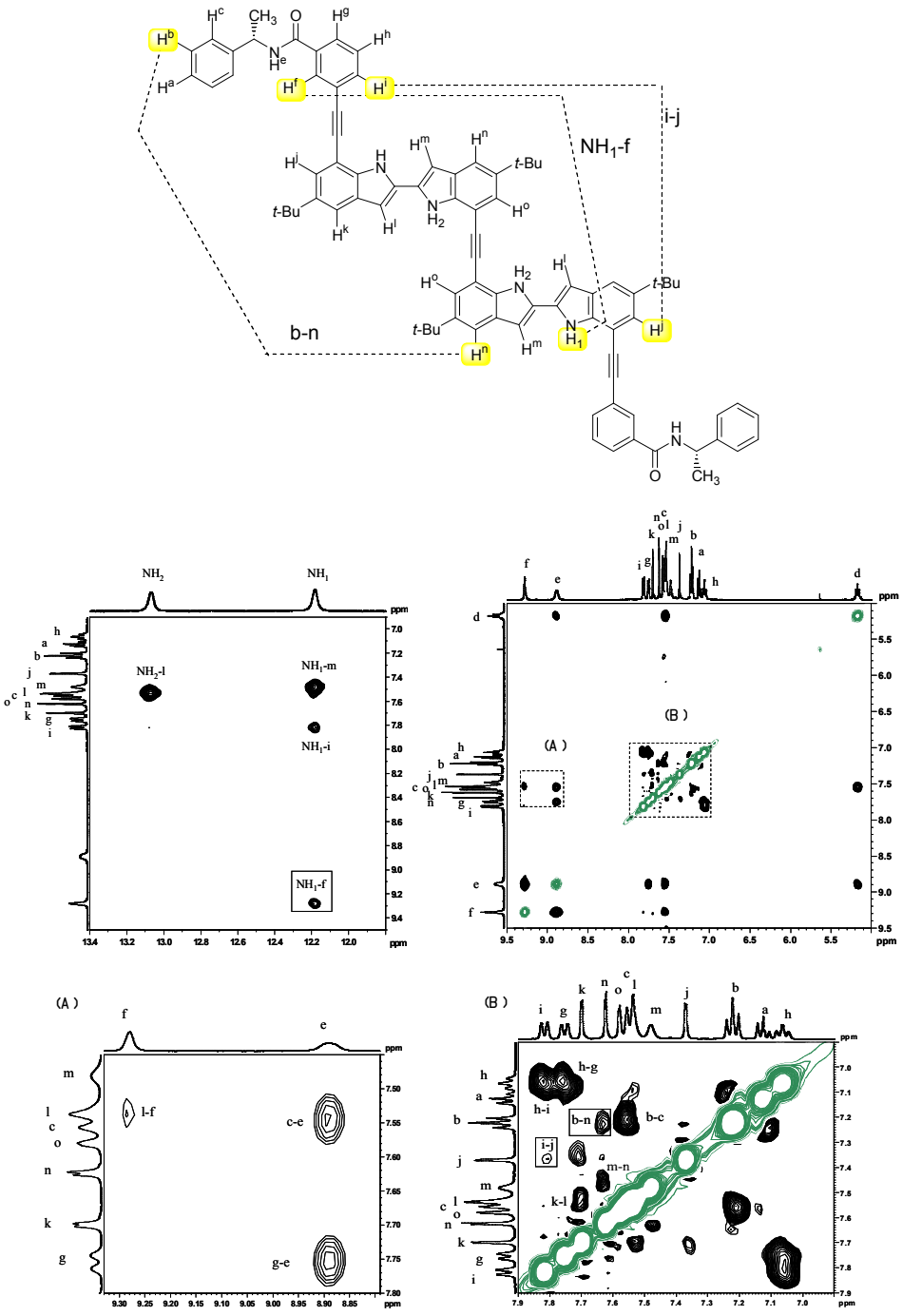

Figure S3. NOESY specta (400 MHz, 25 ^{o}C, acetone-d_6, mixing time = 600 ms) of a mixture of **8a** (10 mM) and $TBA^{+}Cl^{-}$ (3 equiv).

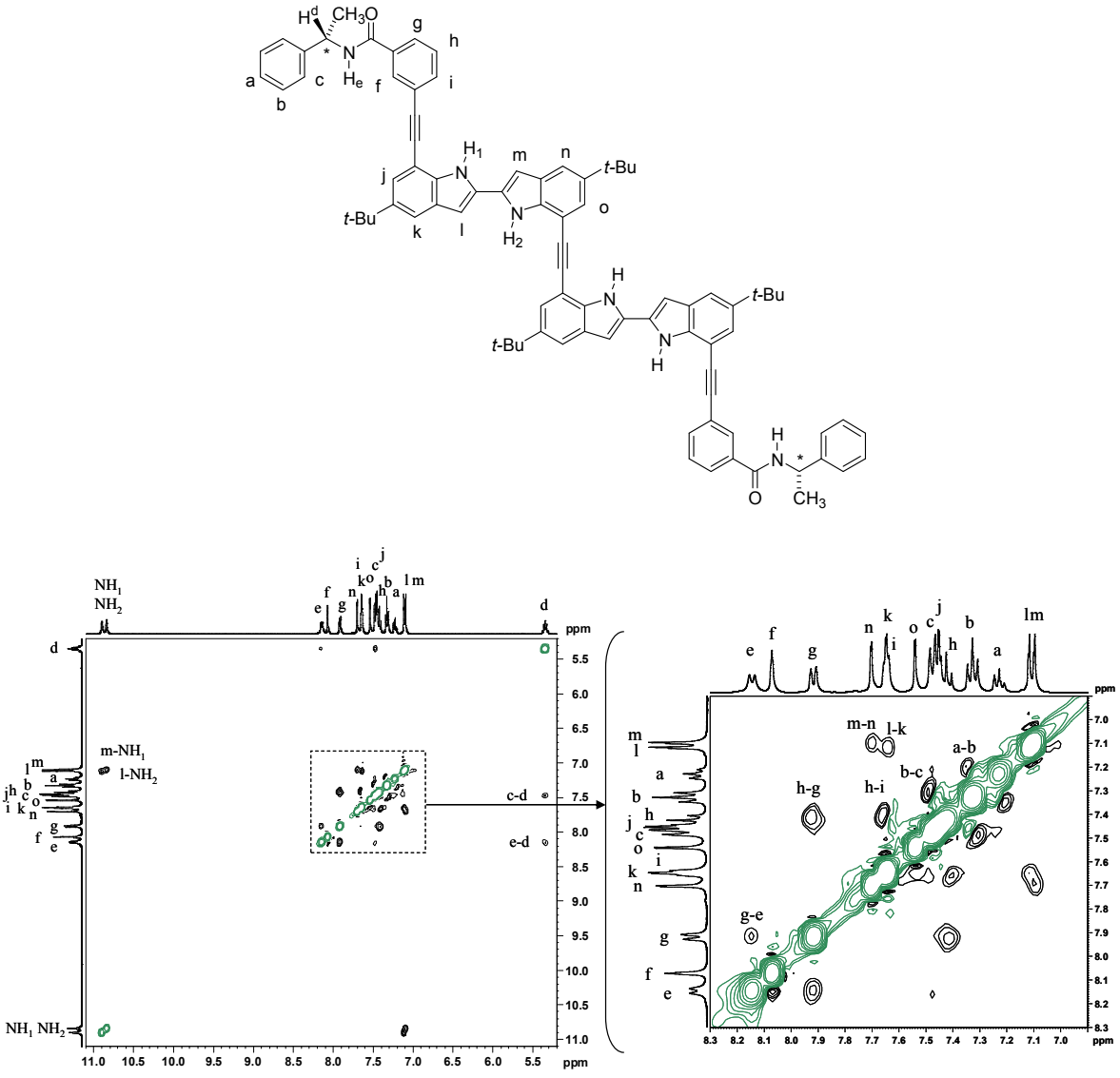

Figure S4. NOESY spectra (400 MHz, 25 ^{o}C, acetone-d_6, mixing time = 600 ms) of **8a** (10 mM) in the absence of an anion, which shows no long distance NOE cross peak.

3. Circular Dichroism (CD) Spectra:[3]

Stock solutions (5.0×10^{-5} M) of **8a** and **8b** were prepared with and without tetrabutylammonium anion ($TBA^+N_3^-$, TBA^+Br^-, TBA^+Cl^-, $TBA^+NO_3^-$ or TBA^+I^-) in CH_2Cl_2. The CD spectra were taken with conditions (scanning rate: 50 nm min^{-1}, bond width: 1 nm, response time: 0.5 sec, accumulations: 3 scans)

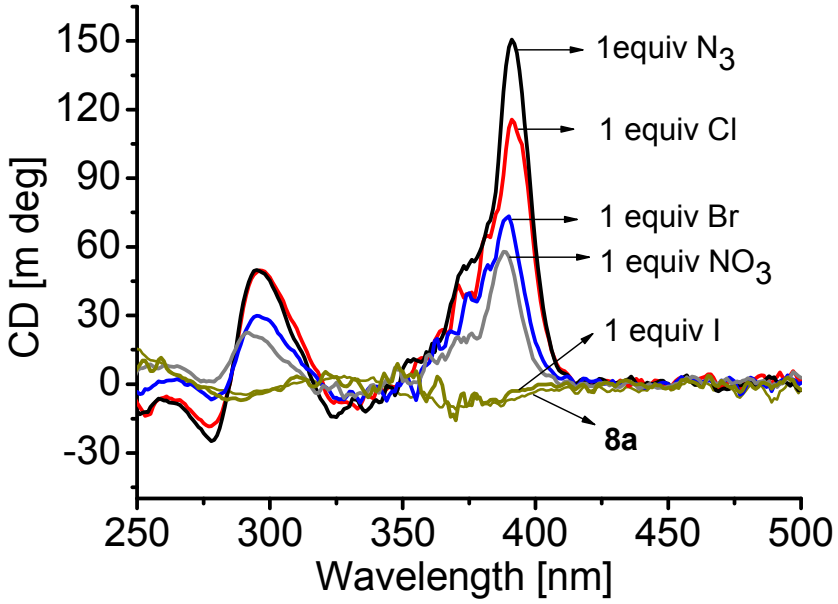

Figure S5. CD spectra of **8a** in the presence of TBA anions in CH_2Cl_2 at 25 ± 1 °C.

[3] a) Rodger, A.; Norden, B. Circular Dichroism and Linear Dichroism, Oxford University Press, Oxford, **1997.** b) Berova, N.; Nakanishi, K.; Woody, R. W. Circular Dichroism: Principles and Applications, 2nd ed. Wiley-VCH, New York, **2000.**

4. Theoretical calculation

Calculations were conducted in gas phase using hybrid *ab-initio* methods with the Gaussian 03 package. First, the structure optimization was performed with HF/3-21G method for both cases. Using the optimized structures, we performed single point calculations with B3LYP/3-21G, and MP2/3-21G methods to compare the energy of the helices. This kind of structure optimization-single point hybrid calculation is widely used due to their relatively accurate result, yet inexpensive computation cost. For all three cases (HF/3-21G, HF/3-21G//B3LYP/3-21G, and HF/3-21G//MP2-3-21G), the (*P*)-helix is more stable than the (*M*)-helix as summarized in Table S1.

Table S1. Calculated energy difference ($\Delta E = E_M - E_P$) between the (*M*)-helix and the (*P*)-helix

Method	HF/3-21G	HF/3-21G//B3LYP/3-21G	HF/3-21G//MP2/3-21G
ΔE (kJ/mol)	23.63	19.43	16.30

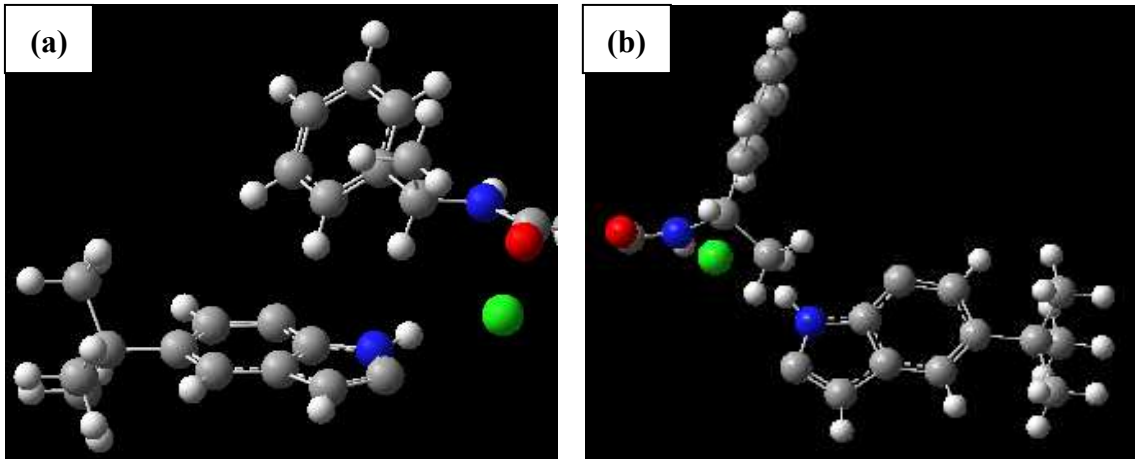

Figure S6. Terminal benzylic portions of the optimized structure for (a) the (*M*)-helix, and (b) the (*P*)-helix. To clarify the relation between the methyl group and indole surface, other atoms are omitted.

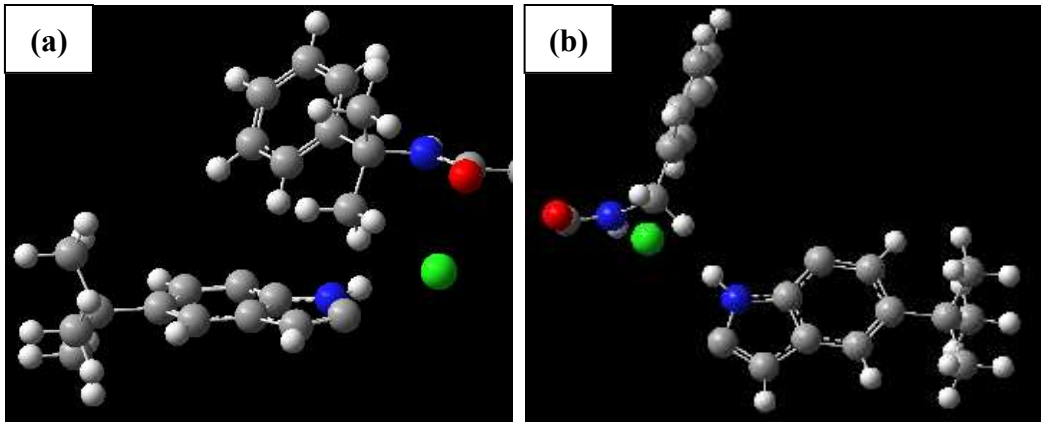

Figure S7. (a) The (*M*)-helix with the benzylic hydrogen substituted to the methyl group, and (b) the (*P*)-helix with the benzylic methyl group substituted to hydrogen. For clarity, some atoms are hidden from view.

In order to verify why the (*P*)-helix has lower energy than the (*M*)-helix, we performed further simulations by changing the group facing the indole surface (Figures S6 and S7). In case of the (*M*)-helix, when the indole surface facing hydrogen was changed to methyl group the energy was greatly stabilized. On the other hand, as the indole surface facing methyl group was substituted to a hydrogen atom, the energy of the (*P*)-helix was greatly destabilized. This indicates the methyl group facing the indole surface experiences strong CH···π interactions which greatly stabilizes the (*P*)- helix . The results are summarized in Table S2.

Table S2. Calculated energy difference between the original helices and the methyl substituted (*M*)-helix and the hydrogen substituted (*P*)-helix. ($\Delta E_M = E_{M\text{-substitued}} - E_M$, $\Delta E_P = E_{P\text{-substitued}} - E_P$)

Method	HF/3-21G	MP2/3-21G
ΔE_M (kJ/mol)	-101,876	-102,154
ΔE_P (kJ/mol)	+101,932	+102,189

5. Binding Studies

Titrations: The experiments were conducted using UV-visible spectroscopy and were all duplicated at 21 ± 1 ^{o}C in 1% (v/v) MeOH in CH_2Cl_2. The stock solution (1.0×10^{-5} M) of **8a** was first prepared. Using this solution as a solvent, a stock solution of an anion (0.3-20 mM, depends on the guest) was prepared. A 2.0 mL of **8a** was transferred to a UV cell, and an initial absorption spectrum was taken. To this solution were added small portions of the anion solution (10 μL initially, then 20-50 μL, and finally 100-200 μL), and the spectrum was recorded after each addition and 12-16 data points were obtained. Upon addition of an anion, the UV-visible spectra were gradually changed, showing multiple isosbestic points at wavelengths. The association constants (K_a) were determined by nonlinear curve fitting of the titration curves[4], plotting the absorbance change at two different wavelengths against equivalents of an anion added.

Job's plots:[5] Stock solutions of the chiral oligomer **8a** (5.0×10^{-5} M) and an anion (5.0×10^{-5} M) were separately prepared in 1% (v/v) MeOH in CH_2Cl_2. The UV-visible spectrum was taken for each of 10 different solutions containing total 1.5 mL of the host and an anion in the following ratios: 1.50:0, 1.35:0.15, 1.20:0.30, 1.05:0.45, 0.90:0.60, 0.75:0.75, 0.60:0.90, 0.45:1.05, 0.30:1.20, and 0.15:1.35.

[4] Long, J. R ; Drago, R. S. *J. Chem. Edu*., **1982**, *59*, 1037-1039.
[5] Connors, K. A. *Binding Constants*, John Wiley & Sons, New York, **1987**, pp. 24–28.

a) 8a + $TBA^+ N_3^-$ **1) Job's plot**

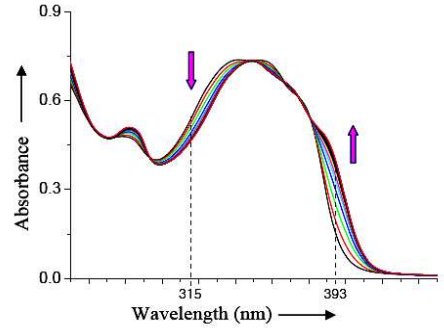

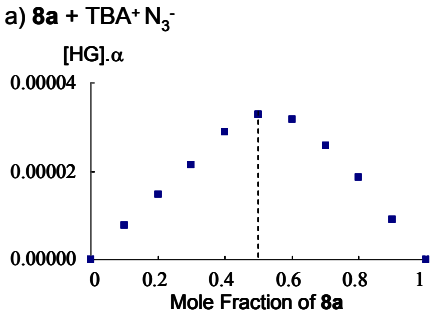

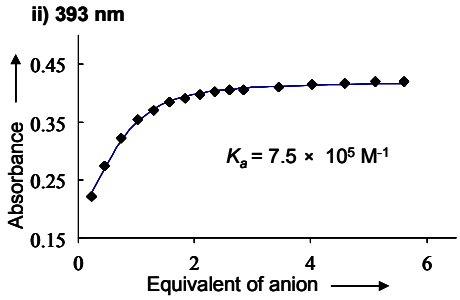

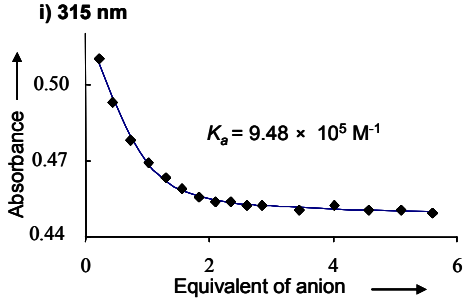

b) 8a + $TBA^+ Cl^-$ **2) Job's plot**

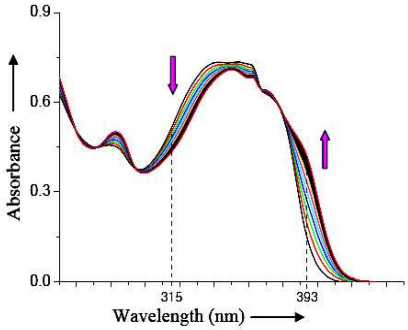

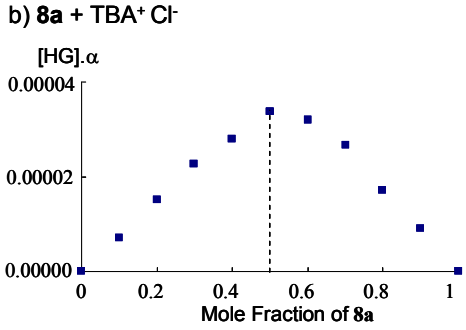

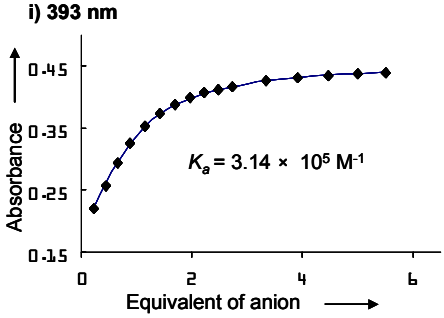

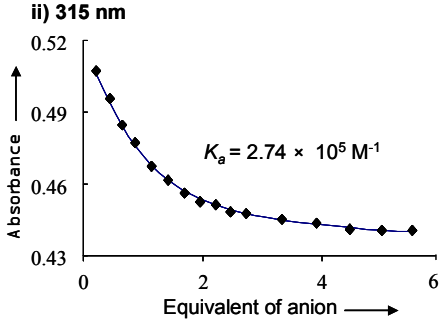

c) 8a + $TBA^+ Br^-$

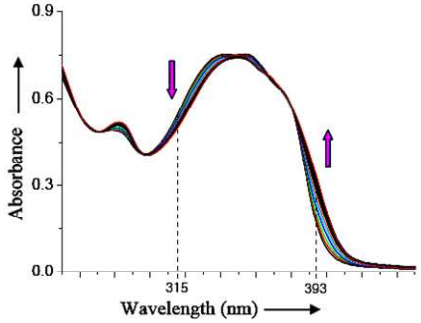

3) Job's plot

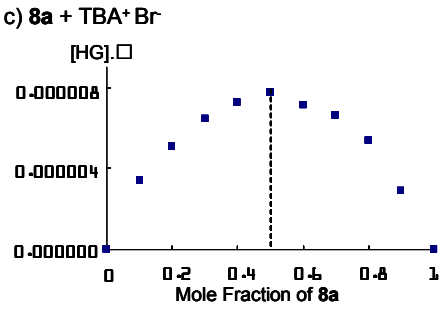

i) 315 nm

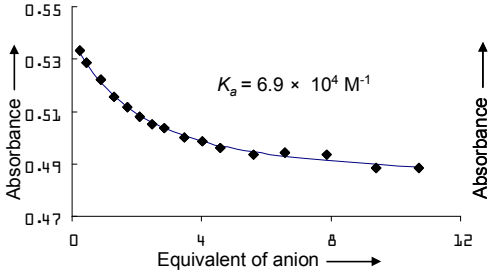

ii) 393 nm

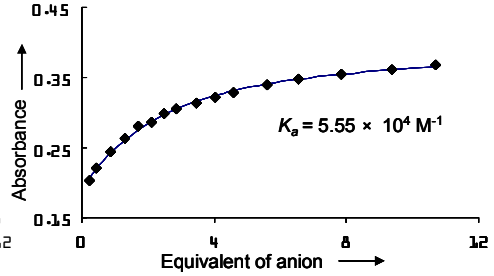

d) 8a + $TBA^+ NO_3^-$

4) Job's plot

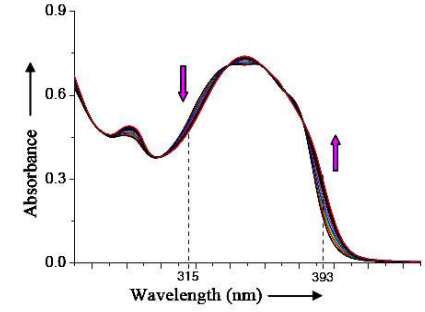

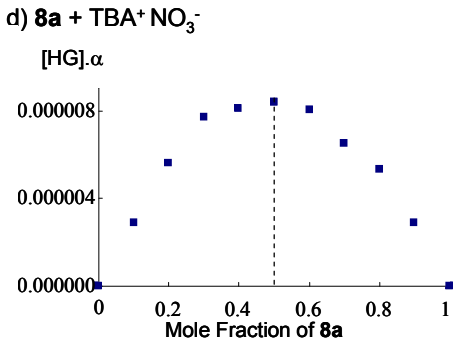

i) 315 nm

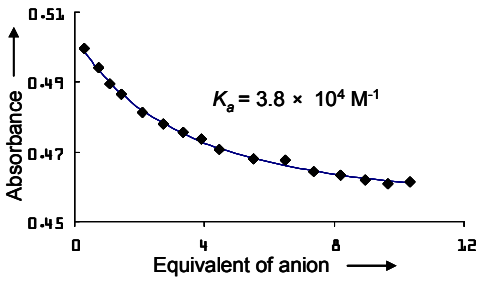

ii) 393 nm

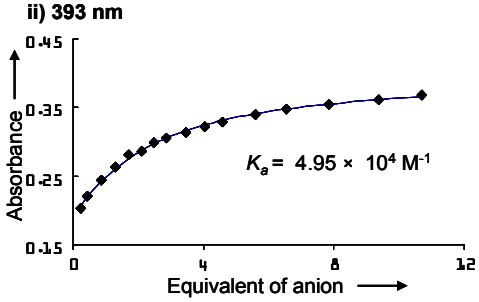

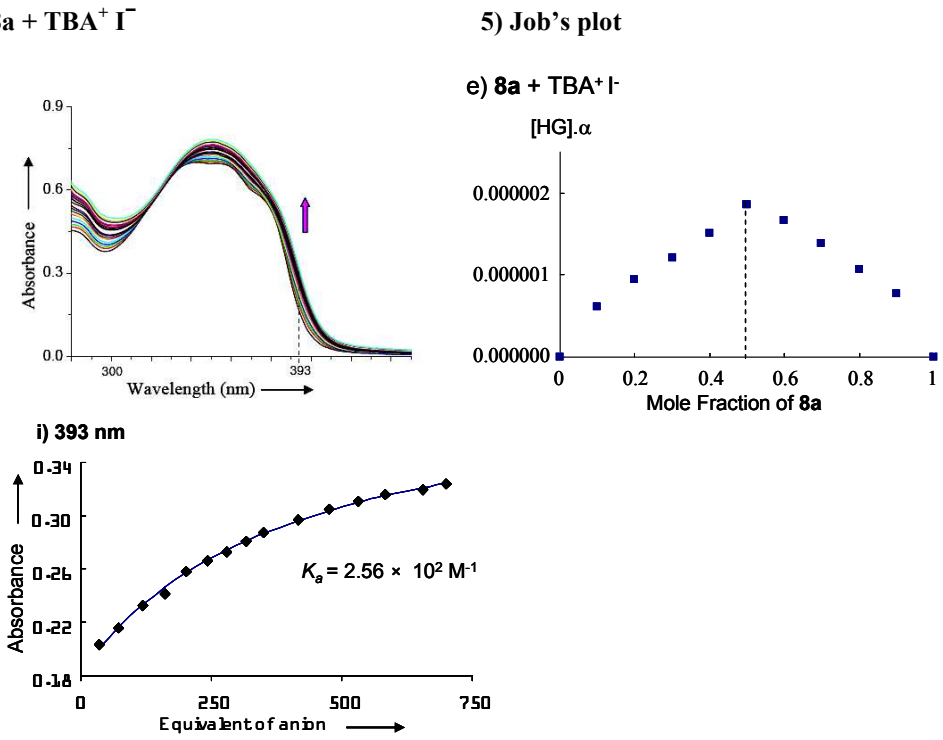

Figure S8. The UV/Vis spectra of **8a** upon addition of anion (top, left), experimental (dots) and theoretical curves(lines) (bottom), and Job's plots (top, right)

6. ^{1}H and ^{13}C NMR spectra of new compounds (400 MHz for ^{1}H and 100 MHz for ^{13}C, DMSO-d_6, 25 °C)

3

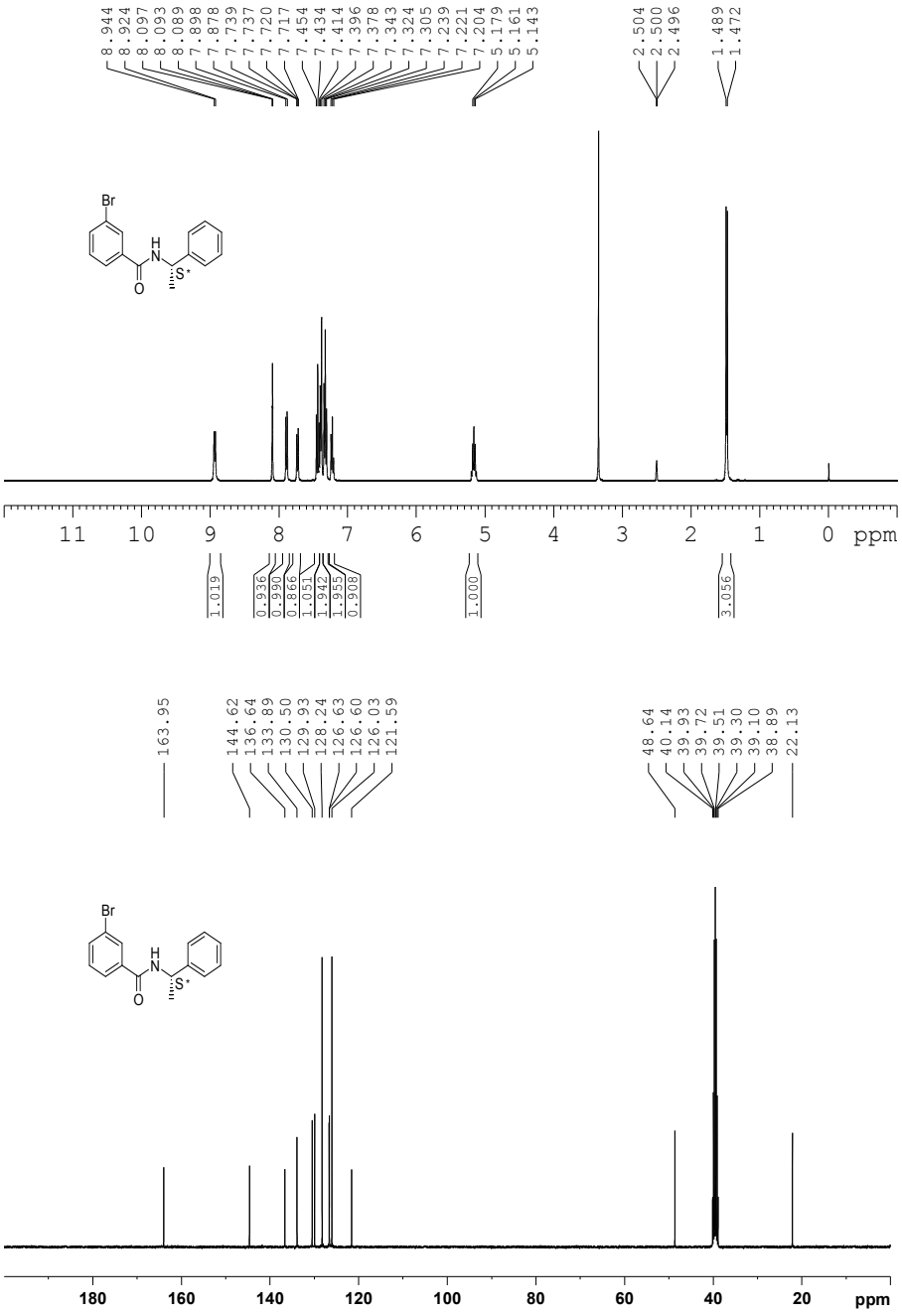

S1

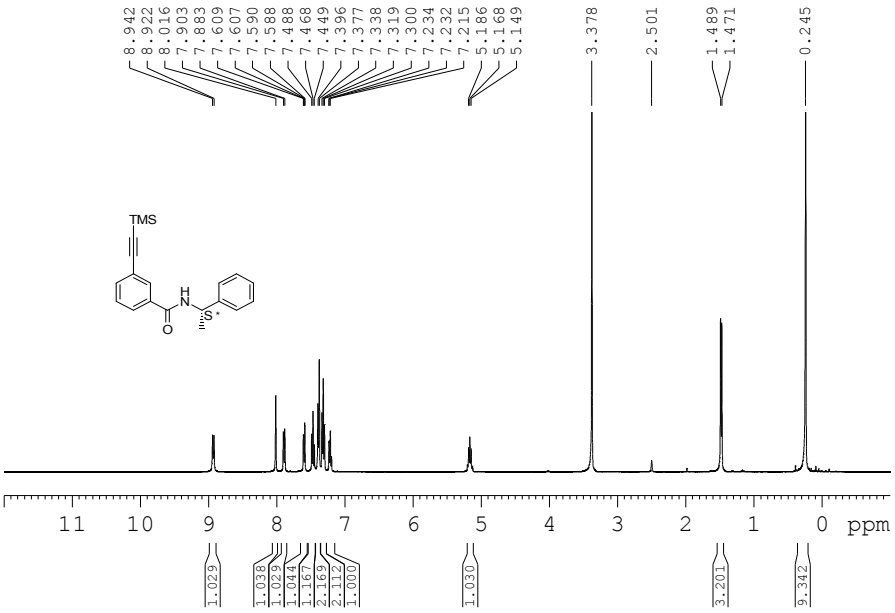
8.942
8.922
8.016
7.903
7.883
7.609
7.607
7.590
7.588
7.488
7.468
7.449
7.396
7.377
7.338
7.319
7.300
7.234
7.232
7.215
5.186
5.168
5.149
3.378
2.501
1.489
1.471
0.245
TMS
11 10 9 8 7 6 5 4 3 2 1 0 ppm
1.029
1.038
1.029
1.044
1.167
2.169
2.112
1.000
1.030
3.201
9.342

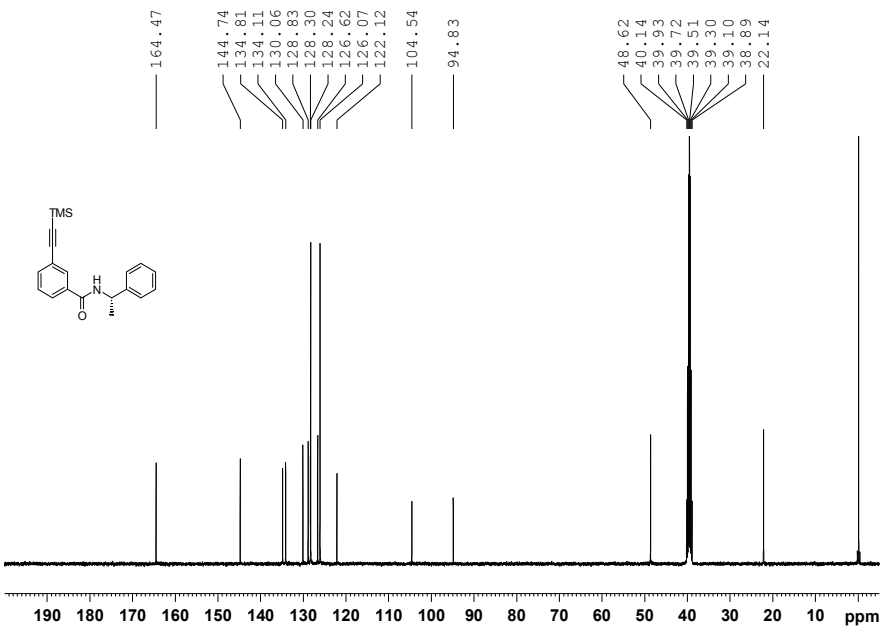
164.47
144.74
134.81
134.11
130.06
128.83
128.30
128.24
126.62
126.07
122.12
104.54
94.83
48.62
40.14
39.93
39.72
39.51
39.30
39.10
38.89
22.14
TMS
190 180 170 160 150 140 130 120 110 100 90 80 70 60 50 40 30 20 10 ppm

4

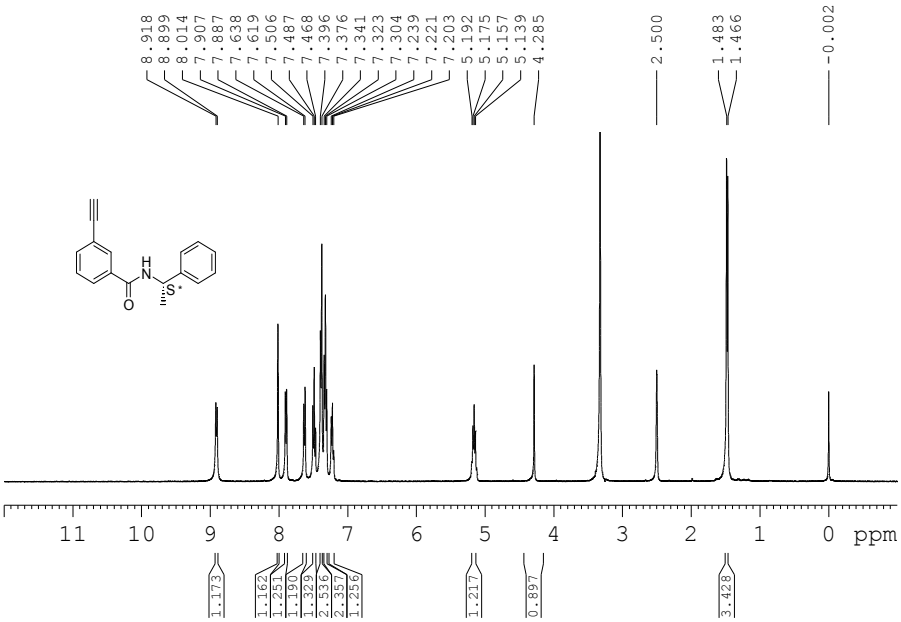
8.918
8.899
8.014
7.907
7.887
7.638
7.619
7.506
7.487
7.468
7.396
7.376
7.341
7.323
7.304
7.239
7.221
7.203
5.192
5.175
5.157
5.139
4.285
2.500
1.483
1.466
0.002
11 10 9 8 7 6 5 4 3 2 1 0 ppm
1.173
1.162
1.251
1.190
1.326
2.536
2.357
1.256
1.217
0.897
3.428

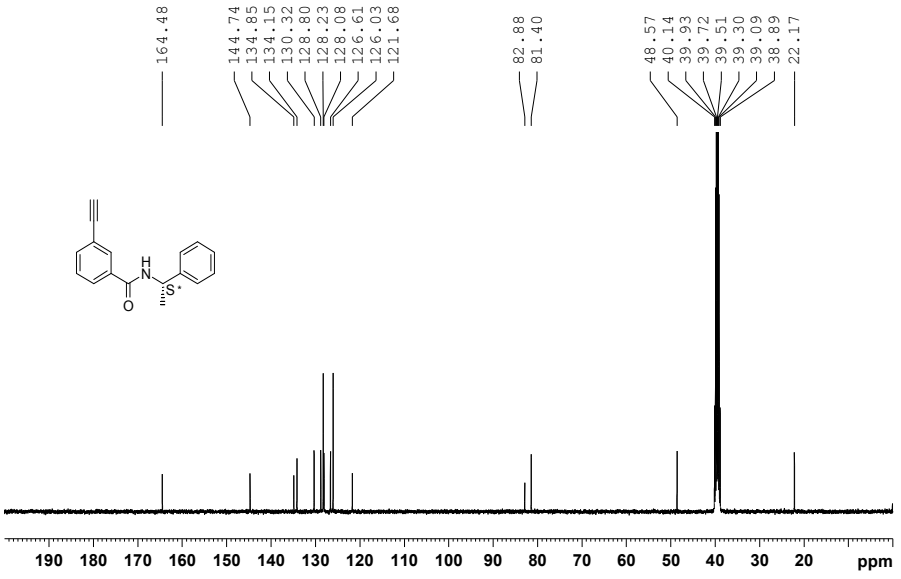
164.48
144.74
134.85
134.15
130.32
128.80
128.23
128.08
126.61
126.03
121.68
82.88
81.40
48.57
40.14
39.93
39.72
39.51
39.30
39.09
38.89
22.17
190 180 170 160 150 140 130 120 110 100 90 80 70 60 50 40 30 20 ppm

6

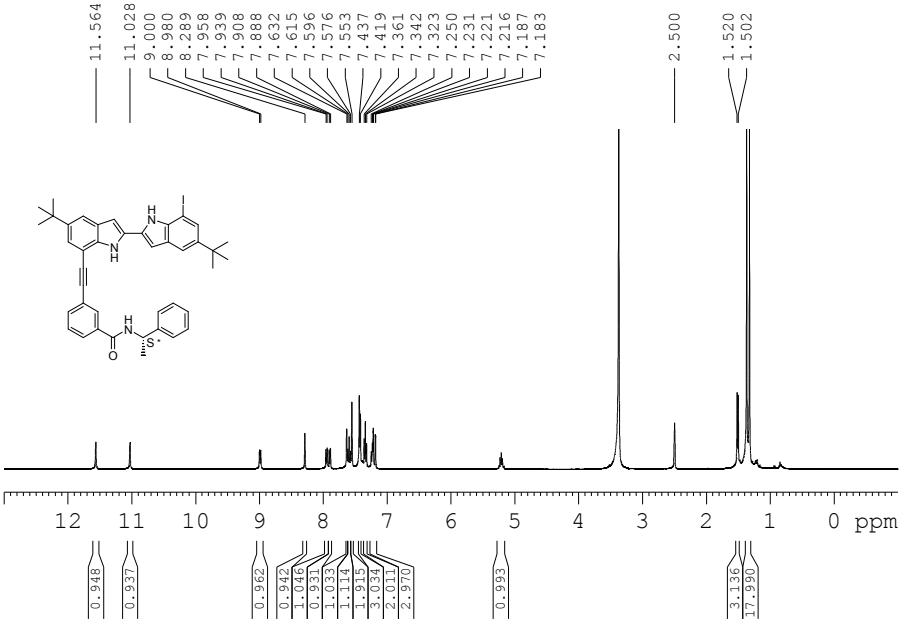
11.564
11.028
9.000
8.980
8.289
7.958
7.939
7.908
7.888
7.632
7.615
7.596
7.576
7.553
7.437
7.419
7.361
7.342
7.323
7.250
7.231
7.221
7.216
7.187
7.183
2.500
1.520
1.502
12 11 10 9 8 7 6 5 4 3 2 1 0 ppm
0.948
0.937
0.962
0.942
1.046
0.931
1.033
1.114
1.915
3.034
2.011
2.970
0.993
3.136
17.990

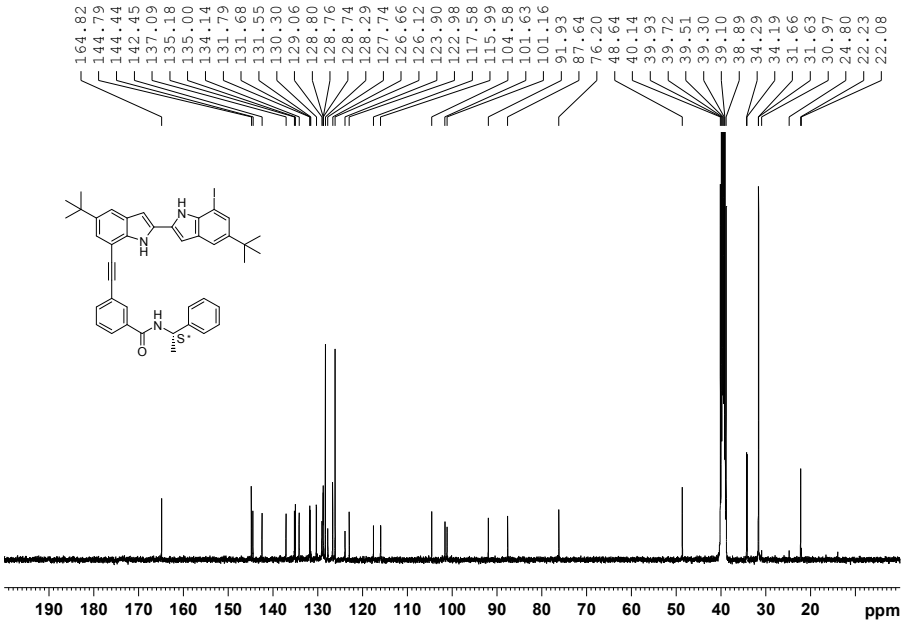
164.82
144.79
144.44
142.45
137.09
135.18
135.00
134.14
131.79
131.68
131.55
130.30
129.06
128.80
128.76
128.74
128.29
127.74
126.66
126.12
123.90
122.98
117.58
115.99
104.58
101.63
101.16
91.93
87.64
76.20
48.64
40.14
39.93
39.72
39.51
39.30
39.10
38.89
34.29
34.19
31.66
31.63
30.97
24.80
22.23
22.08
190 180 170 160 150 140 130 120 110 100 90 80 70 60 50 40 30 20 ppm

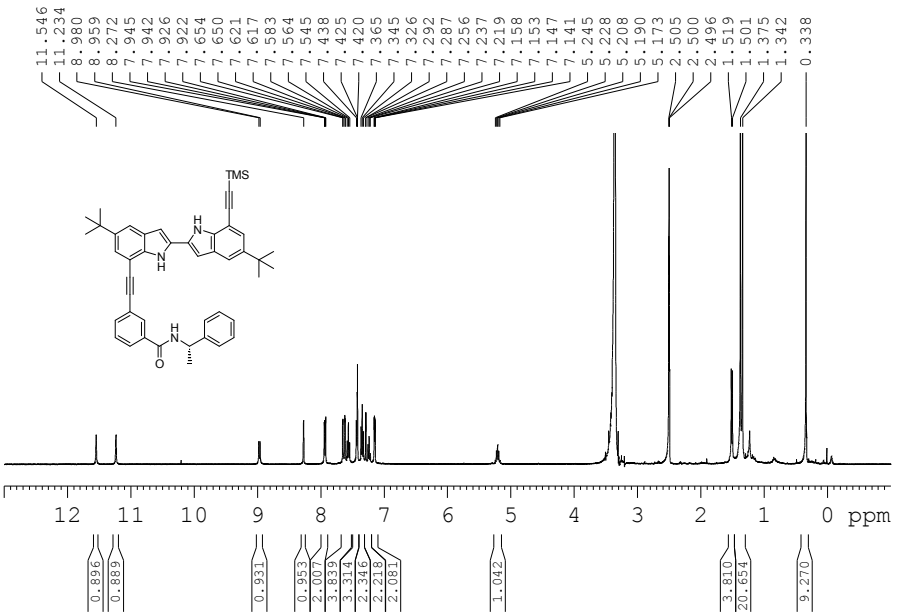
11.546
11.234
8.980
8.959
8.272
7.945
7.942
7.926
7.922
7.654
7.650
7.621
7.617
7.583
7.564
7.545
7.438
7.425
7.420
7.365
7.345
7.326
7.292
7.287
7.256
7.237
7.219
7.158
7.153
7.147
7.141
5.245
5.228
5.208
5.190
5.173
2.505
2.500
2.496
1.519
1.501
1.375
1.342
0.338
TMS
12 11 10 9 8 7 6 5 4 3 2 1 0 ppm
0.896
0.889
0.931
0.953
2.007
3.839
3.314
2.346
2.218
2.081
1.042
3.810
20.654
9.270

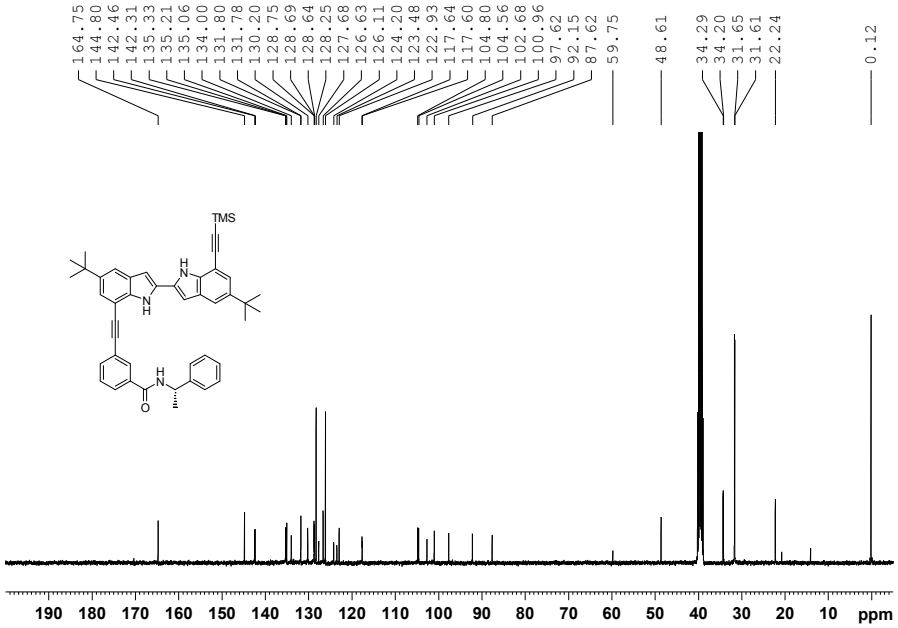
164.75
144.80
142.46
142.31
135.33
135.21
135.06
134.00
131.80
131.78
130.20
128.75
128.69
128.64
128.25
127.68
126.63
126.11
124.20
123.48
122.93
117.64
117.60
104.80
104.56
102.68
100.96
97.62
92.15
87.62
59.75
48.61
34.29
34.20
31.65
31.61
22.24
0.12
TMS
190 180 170 160 150 140 130 120 110 100 90 80 70 60 50 40 30 20 10 ppm

7

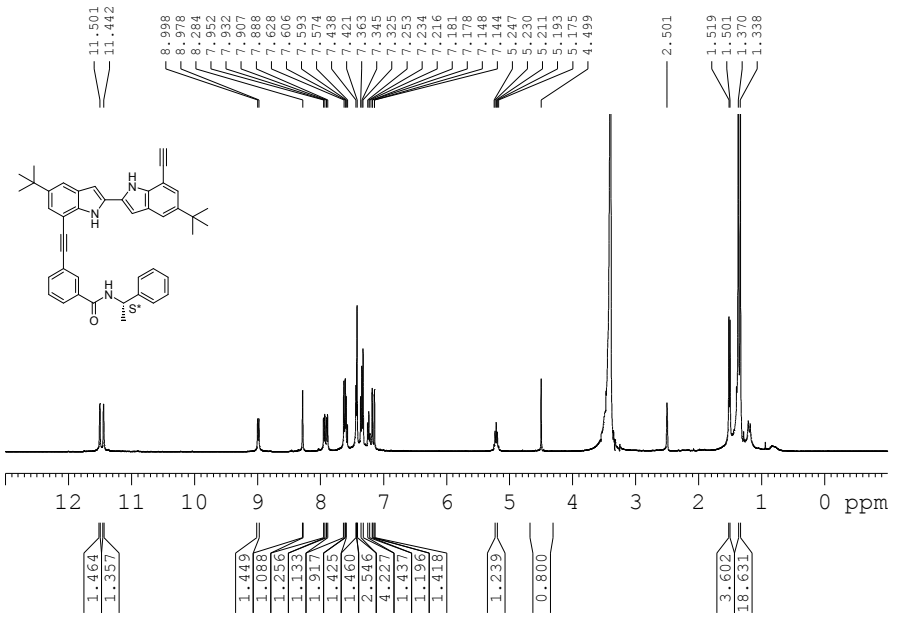
11.501
11.442
8.998
8.978
8.284
7.952
7.932
7.907
7.888
7.628
7.606
7.593
7.574
7.438
7.421
7.363
7.345
7.325
7.253
7.234
7.216
7.181
7.178
7.148
7.144
5.247
5.230
5.211
5.193
5.175
4.499
2.501
1.519
1.501
1.370
1.338
12 11 10 9 8 7 6 5 4 3 2 1 0 ppm
1.464
1.357
1.449
1.088
1.256
1.133
1.917
1.425
1.460
2.546
4.227
1.437
1.196
1.418
1.239
0.800
3.602
18.631

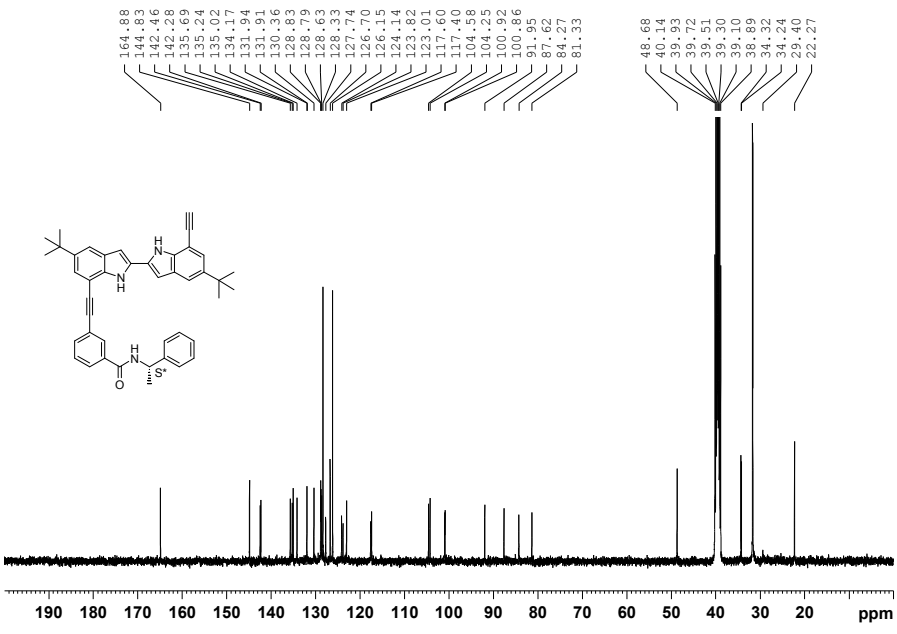
164.88
144.83
142.46
142.28
135.69
135.24
135.02
134.17
131.94
131.91
130.36
128.83
128.79
128.63
128.33
127.74
126.70
126.15
124.14
123.82
123.01
117.60
117.40
104.58
104.25
100.92
100.86
91.95
87.62
84.27
81.33
48.68
40.14
39.93
39.72
39.51
39.30
39.10
38.89
34.32
34.24
29.40
22.27
190 180 170 160 150 140 130 120 110 100 90 80 70 60 50 40 30 20 ppm

8a

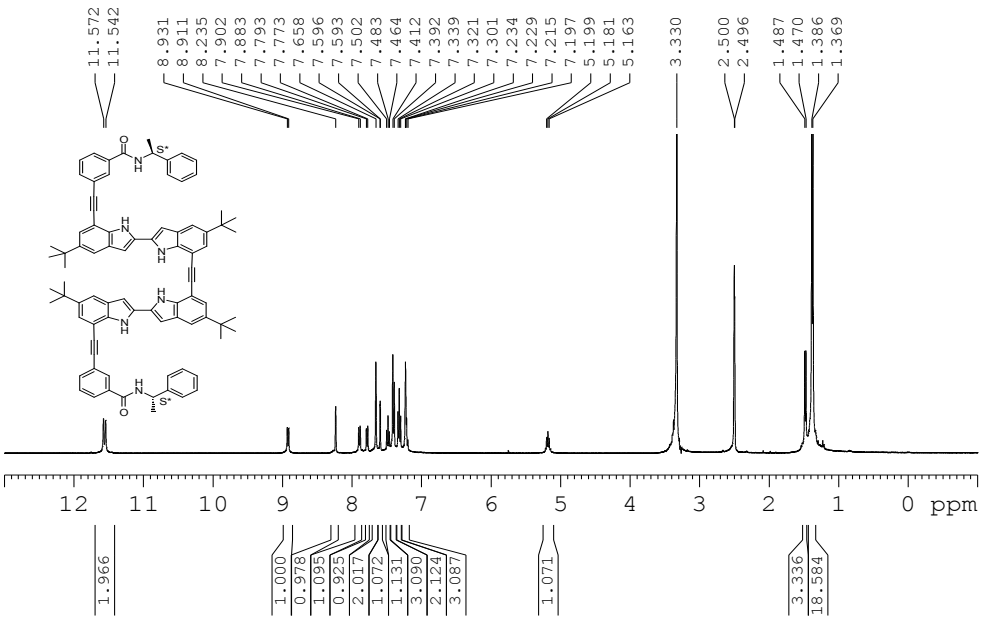
11.572
11.542
8.931
8.911
8.235
7.902
7.883
7.793
7.773
7.658
7.596
7.593
7.502
7.483
7.464
7.412
7.392
7.339
7.321
7.301
7.234
7.229
7.215
7.197
5.199
5.181
5.163
3.330
2.500
2.496
1.487
1.470
1.386
1.369
12 11 10 9 8 7 6 5 4 3 2 1 0 ppm
1.966
1.000
0.978
1.095
0.925
2.017
1.072
1.131
3.090
2.124
3.087
1.071
3.336
18.584

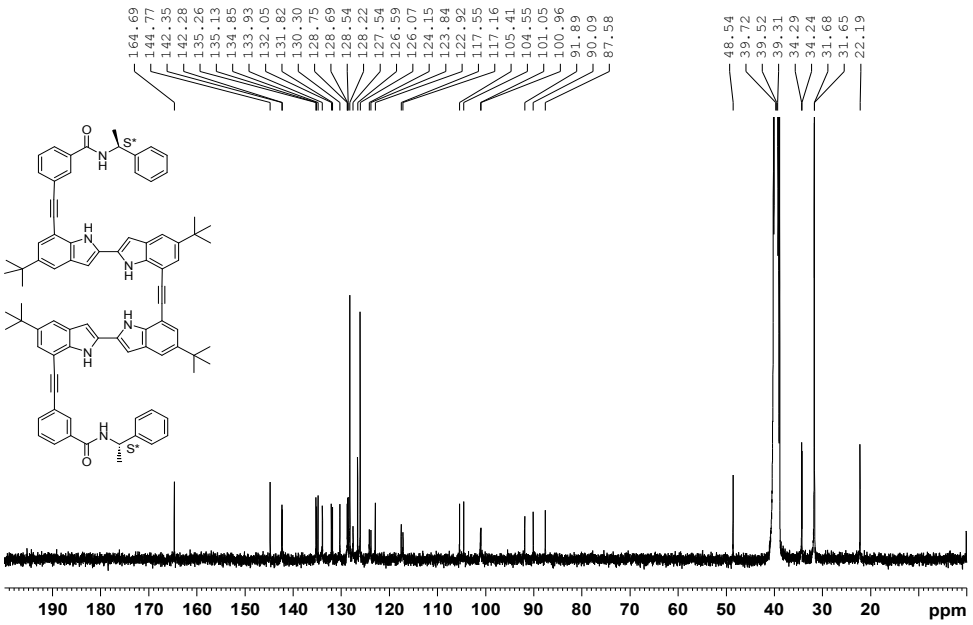
164.69
144.77
142.35
142.28
135.26
135.13
134.85
133.93
132.05
131.82
130.30
128.75
128.69
128.54
128.22
127.54
126.59
126.07
124.15
123.84
122.92
117.55
117.16
105.41
104.55
101.05
100.96
91.89
90.09
87.58
48.54
39.72
39.52
39.31
34.29
34.24
31.68
31.65
22.19
190 180 170 160 150 140 130 120 110 100 90 80 70 60 50 40 30 20 ppm

8b

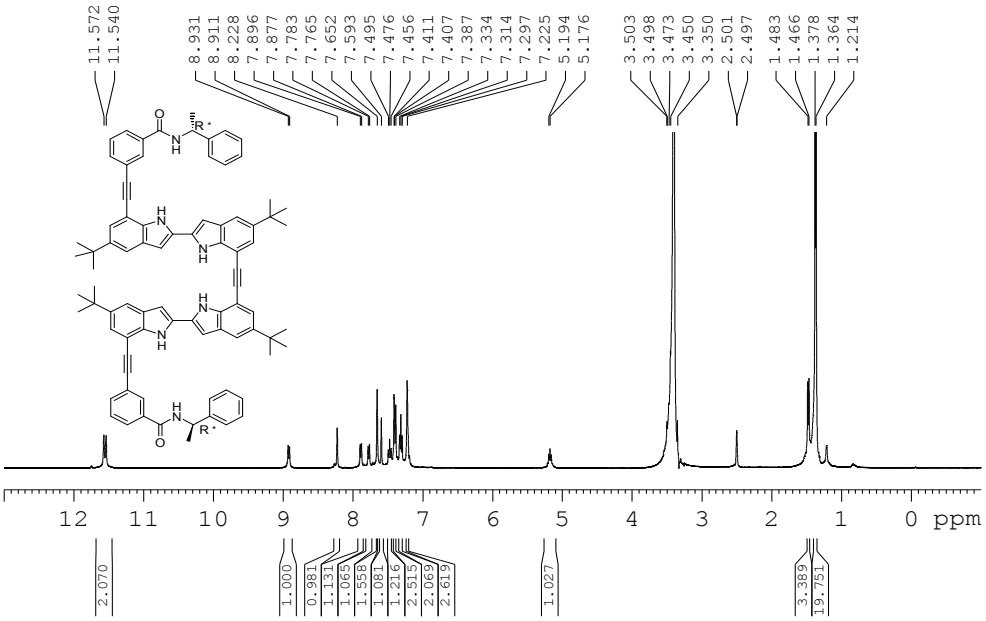
11.572
11.540
8.931
8.911
8.228
7.896
7.877
7.783
7.765
7.652
7.593
7.495
7.476
7.456
7.411
7.407
7.387
7.334
7.314
7.297
7.225
5.194
5.176
3.503
3.498
3.473
3.450
3.350
2.501
2.497
1.483
1.466
1.378
1.364
1.214
12 11 10 9 8 7 6 5 4 3 2 1 0 ppm
2.070
1.000
0.981
1.131
1.065
1.558
1.081
1.216
2.515
2.069
2.619
1.027
3.389
19.751

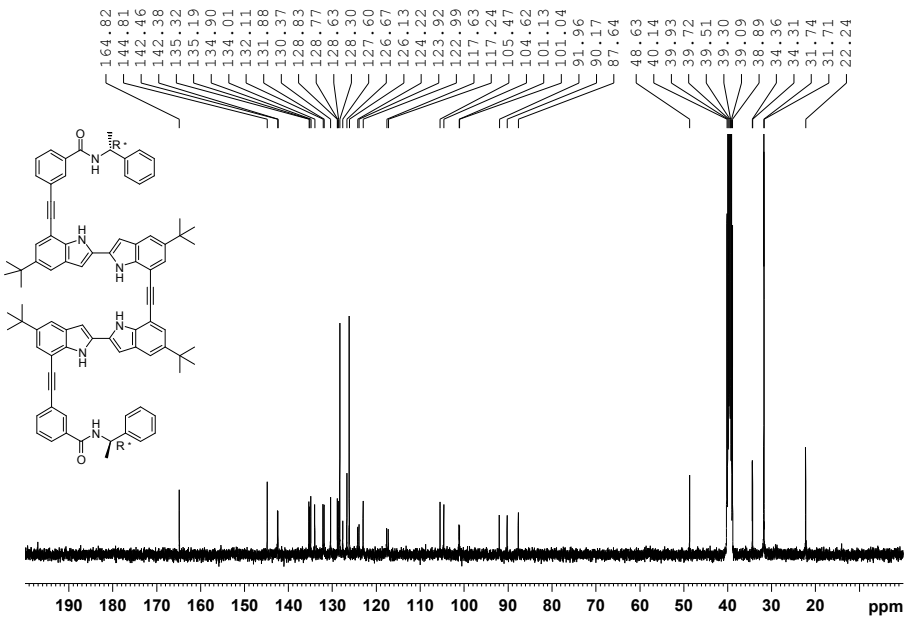
164.82
144.81
142.46
142.38
135.32
135.19
134.90
134.01
132.11
131.88
130.37
128.83
128.77
128.63
128.30
127.60
126.67
126.13
124.22
123.92
122.99
117.63
117.24
105.47
104.62
101.13
101.04
91.96
90.17
87.64
48.63
40.14
39.93
39.72
39.51
39.30
39.09
38.89
34.36
34.31
31.74
31.71
22.24
190 180 170 160 150 140 130 120 110 100 90 80 70 60 50 40 30 20 ppm